



International Conference on Advances in Manufacturing and Materials Engineering,
AMME 2014

Effect of Warm Rolling on the Evolution of Microstructure, Microtexture and Mechanical Properties of Commercial Grade Duplex Steel

B. Bhadak, M. Zaid, P.P. Bhattacharjee*

*Department of Materials Science and Engineering, Indian Institute of Technology Hyderabad, Ordnance Factory Estate, Yeddumailaram
502205, AP India*

Abstract

The effect of warm rolling on the evolution of microstructure, microtexture and mechanical properties of a duplex stainless steel (DSS) was investigated. For this purpose, the DSS alloy was warm rolled at 625°C up to 90% reduction of thickness. Development of ultrafine lamellar morphology with alternate arrangement of the two phases was revealed during warm rolling. The ferrite in DSS developed stronger RD-fiber (RD//<110>) than ND-fiber (ND//<111>) while austenite in DSS showed pure metal or copper type texture. The DSS in the as warm-rolled condition showed tremendous increase in ultimate tensile strength to ~1.4GPa. The present results demonstrate that warm rolling can be used successfully for developing ultrahigh strength DSS.

© 2014 Elsevier Ltd. This is an open access article under the CC BY-NC-ND license

(<http://creativecommons.org/licenses/by-nc-nd/3.0/>).

Selection and peer-review under responsibility of Organizing Committee of AMME 2014

Keywords: DSS; warm rolling; microstructure; EBSD; microtexture; texture

Introduction:

Duplex stainless steels are ferritic-austenitic steels developed to combine the properties of both ferritic and austenitic grade of steels. DSS have good strength, high toughness, excellent corrosion resistance to corrosion and

* Corresponding author. Tel.: +91 40 2301 6069; fax: +91 40 2301 6032.

E-mail address: pinakib@iith.ac.in

good weldability (Gosh S.K. et al, 2012). Thus, these steels find extensive applications in heat exchangers, pressure vessels, storage tanks, impellers, shafts in chloride environment and sea water systems (Gunn R 1997).

Majority of studies on these alloys have focused on improving corrosion resistance, however, for expanding the usage of these steels in for a wide range of structural applications the deformation behaviour of these steels is to be understood in depth. However, only limited studies have been carried out in this direction (Keichel J et al. 2003). Recently, Bhattacharjee et al have studied warm rolling of custom grade DSS and indicated the possibility of using warm-rolling as a novel thermo-mechanical processing route for DSS alloys (Bhattacharjee P.P. et al, 2013). However, effect of warm rolling of on commercial grade DSS have not been investigated but remain quite interesting. This work contributes to understanding the effect of warm rolling on microstructure, texture and mechanical properties of a commercial grade DSS i.e. SAF 2507.

Experimental:

2.1 Thermo-mechanical Processing:

A commercial grade of DSS with chemical composition shown in Table 1 was subjected to homogenization treatment at 1150°C for two hours using a conventional tubular furnace in argon atmosphere. Samples for warm-rolling having dimensions 20mm (width) by 40mm (length) were machined out from the homogenized material and warm rolled at 625°C in steps of 20%, 40%, 70%, 80% to 90% reduction in thickness using a laboratory scale rolling mill (SPX Precision Equipment, USA) having roll diameter of 140mm. The rolls were preheated to minimize sudden quenching during warm rolling. The samples were quenched immediately after every warm rolling pass.

Table 1: Chemical composition of the experimental DSS

Element	C	S	Cr	Mn	Ni	P	Si	Mo	Fe
Wt. %	0.05	0.001	22.1	2.03	5.48	0.009	0.45	3.05	Balance

2.2 Characterization:

The microstructure and microtexture of the deformed materials were characterized using electron back scatter diffraction (EBSD) system (Oxford Instruments, UK) attached to a FEGSEM (Make: Carl Zeiss, Germany, Model: SUPRA-40). Samples for EBSD were prepared by careful mechanical polishing followed by electro-polishing using a solution of 700ml ethanol, 120 ml distilled water, 100 ml glycerol, and 80 ml perchloric acid at room temperature. Several EBSD scans were performed on the RD-ND plane close to the mid thickness region EBSD data acquired from centre of to ensure the plain strain condition. Acquired scans were merged to get statistically reliable results. A fine scan step size of 50nm was used. The acquired EBSD dataset were analysed using TSL-OIMTM analysis software. A cut-off angle of 15° used to calculate the volume fraction of different texture components.

Tensile specimens were prepared along the RD as shown schematically in Fig.1. Tensile testing was carried

out using a universal testing machine (Model: 5967 Instron, 30kN load cell, UK) at the strain rate of 10^{-3} sec^{-1} and the loading direction was along the RD. Samples after tensile fracture were cut in such a way that EBSD could be carried out at the vicinity of the neck region.

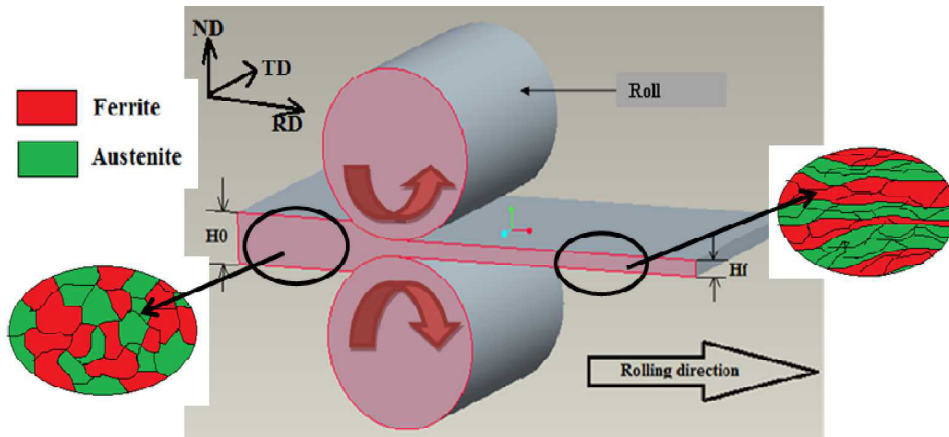


Fig.1. Schematic of rolling of sheet with microstructure in RD-ND plane of rolling

3. Results:

Figure 2(a) shows the phase map of homogenized DSS at 1150°C . Even after homogenization prior elongated morphology of the hot rolled microstructure is retained. During homogenization, the austenite volume fraction (A_f) of $\sim 40\%$ is achieved. Average grain size measured along the ND is nearly $\sim 9\mu\text{m}$ for both the phases. Comparison of the $\phi_2=45^\circ$ section of the orientation distribution function (ODF) of ferrite (Fig.2(c)) with that of the ideal ODF section (Fig.2(g)) shows the presence of stronger RD-fiber (RD// $\langle 110 \rangle$) having a volume fraction of $\sim 31\%$ as compared to the ND-fiber (ND// $\langle 111 \rangle$) with volume fraction $\sim 7\%$. Comparison of the (111) pole figure of austenite (Fig.2(b)) with that of the ideal pole figure shows the development of pure metal or copper type texture characterized by the presence of copper or Cu ($\{112\}\langle 111 \rangle$; $\sim 6.7\%$), S ($\{123\}\langle 634 \rangle$; $\sim 18.2\%$) and brass or B_S ($\{110\}\langle 112 \rangle$; $\sim 13.3\%$) components.

During warm rolling the two phases are arranged in an alternate banded morphology. The austenite volume fraction remains stable although the deformation processing. The phase map shows that the phase bands are further subdivided by HAGBs (shown in black). With increasing strain the phase band thickness and the HAGB thickness along the ND are reduced (Fig.3). Figures 4(a) and 4(b) show the grain boundary (GB) maps of warm rolled ferrite and austenite, respectively. Formation of substructure is evidenced inside individual phase bands. The point to origin misorientation plots along the arrow marks in individual phase bands are calculated (Fig.4(c)(d)) which shows lower accumulated misorientation in both the phases. Both RD and ND fiber are strengthened during warm rolling as shown in figure 5(a). However, the RD-fiber dominates the texture of ferrite in warm rolled DSS. Austenite in DSS retains the pure metal type texture and is further strengthened during warm rolling (Fig.5(b)).

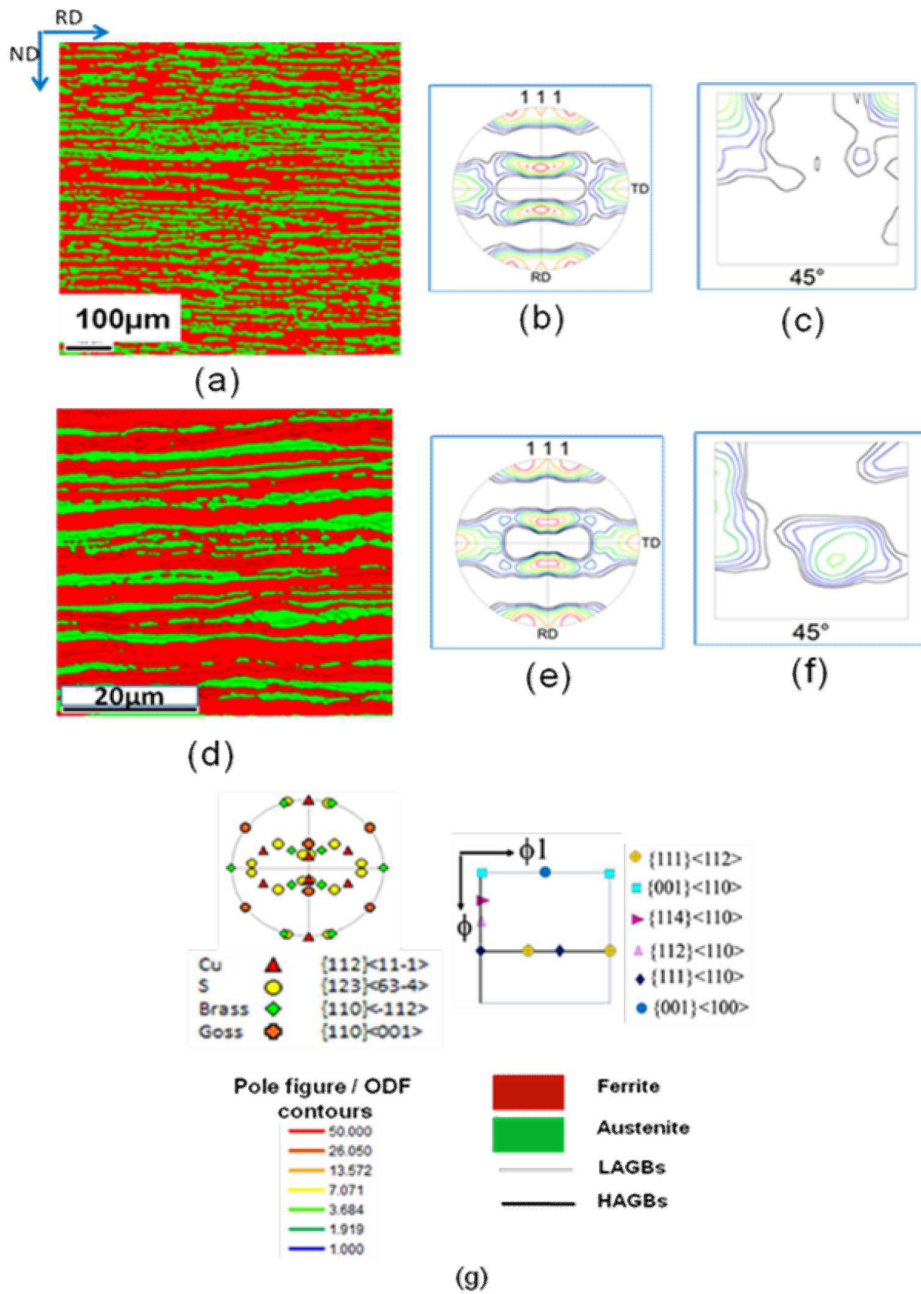


Fig.2: (a) Phase map of homogenized DSS, (b) (111) pole figure of austenite and (c) $\phi_2=45^\circ$ section of the ODF of ferrite in homogenized DSS; (d) Phase map of 90% warm rolled DSS, (e) (111) pole figure of austenite and (f) $\phi_2=45^\circ$ section of the ODF of ferrite in warm rolled DSS; (g) Ideal(111) pole figure of austenite and $\phi_2=45^\circ$ section of ODF of ferrite.

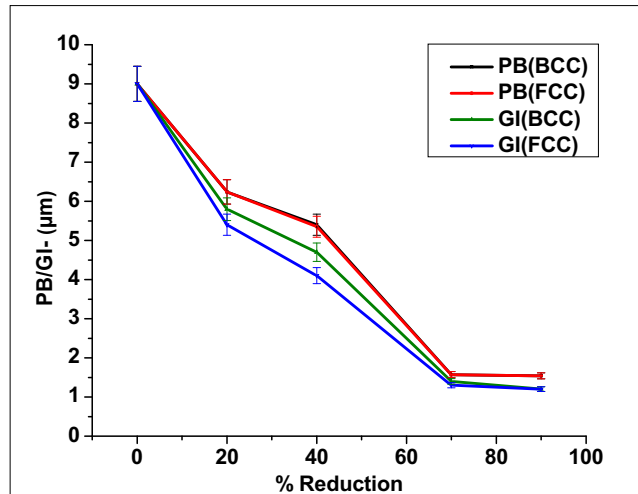
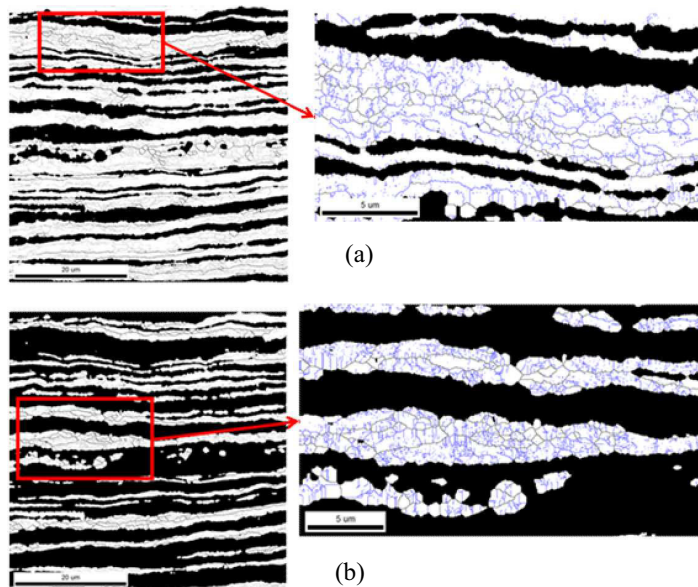


Fig.3. Phase band (PB) and HAGB intercept (GI) vs % reduction along ND

Figure 6(a) shows the stress-strain plot of the as warm rolled DSS specimen. Remarkable increase in the 0.2% offset yield strength to ~1.25GPa and ultimate tensile strength to ~1.4GPa is achieved with considerable elongation ~12%. Fig.6(b) shows the schematic of the fractured specimen. The band contrast map of same region shows existence of deep phase bands. Lamellar bands during plastic flow converged towards necking region.



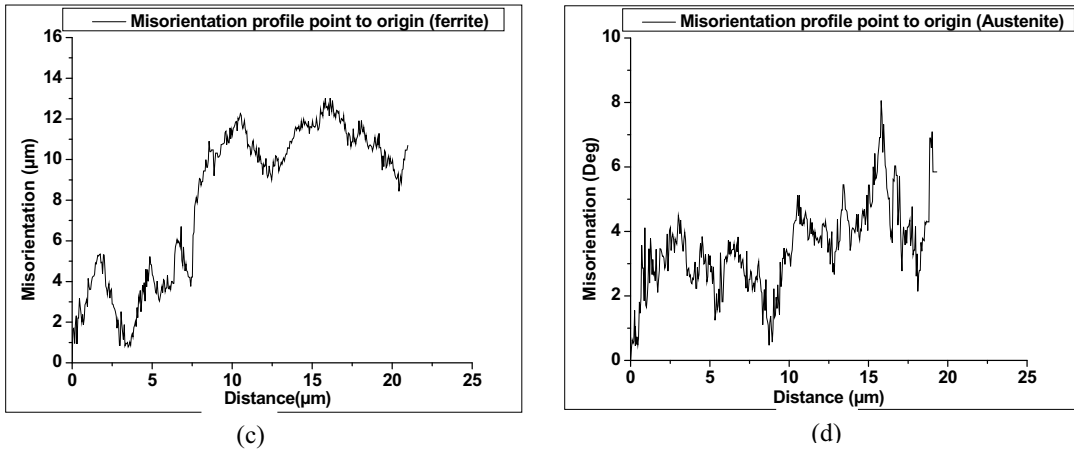


Fig.4. GB maps of (a) ferrite and (b) austenite in DSS; accumulated misorientation profile of (c) ferrite and (d) austenite

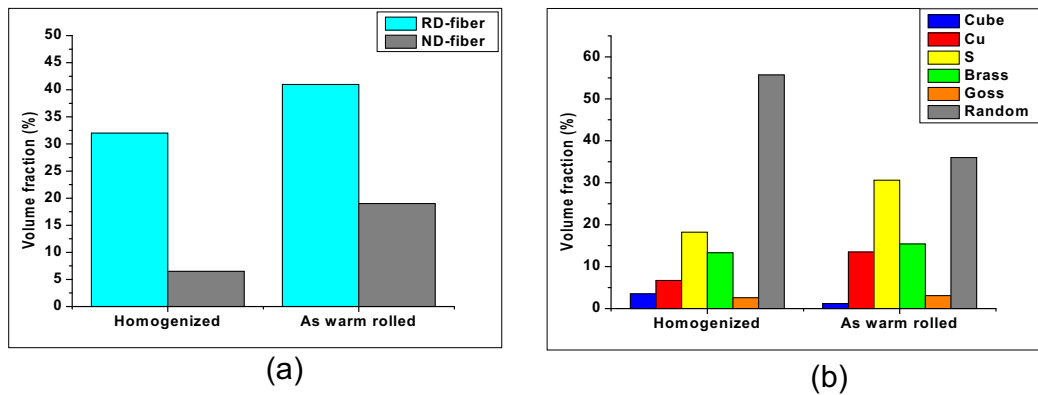


Fig.5. Variation of texture components in (a) ferrite and (b) austenite in DSS.

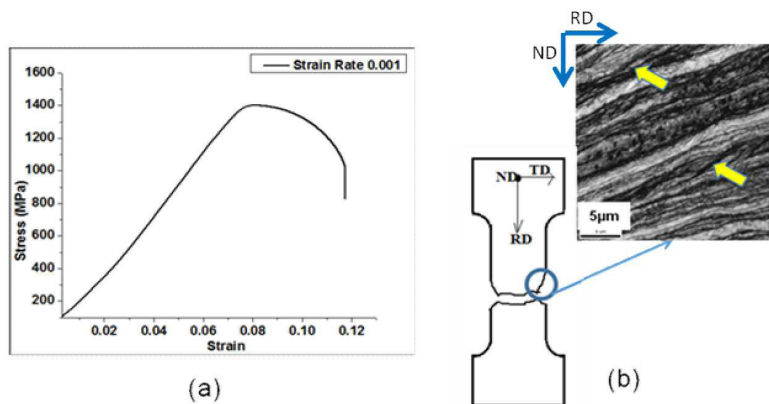


Fig.6. (a) stress-strain plot of as warm rolled DSS (b) schematic of the fractured specimen and IQ map at the vicinity of the necking region.

4. Discussion:

During warm rolling the phase bands align themselves along the RD resulting in an alternate lamellar morphology of the two phases which is also observed in a customized grade of DSS alloy recently reported by Bhattacharjee et al (Bhattacharjee P.P. et al, 2013). With increasing strain subdivision of phase bands by HAGBs results in lower value of HAGB spacing than that of phase band thickness (Fig.3). Misorientation build up inside the bands indicate extensive dynamic recovery (Fig.4(c)).

Both RD and ND fiber are strengthened in ferrite of DSS during warm rolling similar to the behaviour of single phase ferrite as well as ferrite in DSS warm-rolled at the same temperature (Bhattacharjee P.P. et al, 2013). The development of pure metal type texture Austenite is attributed to the increased SFE at the warm-rolling temperature due to which deformation twin formation is suppressed (Latanision R.M. et al, 1971 & Smallman R.E. et al, 1964).

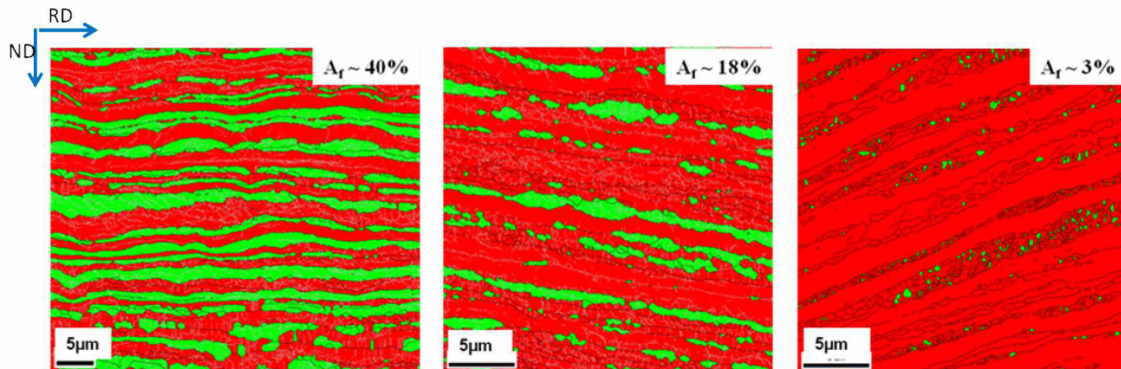


Fig.7 Phase maps showing variation of austenite fraction at different regions (a) as warm rolled (b) 150 μ m and (c) 10 μ m away from the fractured surface in vicinity of necking region

The remarkable increase in strength during warm rolling is attributed to the formation of ultrafine structure and phase bands which act as additional barrier to dislocation motion. As, tensile test is carried out along RD all phase bands are aligned parallel to the tensile axis. One crucial observation is that at the vicinity of the necked region there is gradual decrease in austenite content. Austenite fraction of 40% in the as warm rolled DSS is reduced drastically to ~18% at the region 150 μ m away from fractured surface and is further reduced to just 3% at 10 μ m away from fracture (Fig.7). This possibly indicates that austenite is transformed to martensite (which is indexed as a bcc phase during EBSD measurements) locally due to stress concentration in the necked region. Indirect evidence of this is obtained from the IQ map obtained at the vicinity of the necked region which shows great variation in the IQ distribution in the ferrite phase. However, further studies need to be carried out to fully clarify the implications of this phenomenon on the evolution of mechanical properties.

5. Conclusion:

1. Ultra-fine microstructure with alternate arrangement of ferrite and austenite bands is developed during heavy warm rolling of DSS.
2. During warm rolling of DSS both RD and ND-fiber components are strengthened in ferrite. Austenite shows pure metal type texture due to suppression of deformation twinning.
3. Ultra high strength obtained of warm rolled DSS possibly originate from formation of ultrafine microstructure and possible role of finely spaced phase boundaries as additional barriers to dislocation motion.
4. The present results demonstrate that warm rolling can be used successfully for developing ultrahigh strength DSS

References:

Gosh S.K. et al, 2012, Effect of rolling deformation and solution treatment on microstructure and mechanical properties of a cast duplex stainless steel Bull. Mater. Sci., vol. 35, pp. 839-846.

Gunn R., 1997, Duplex stainless steels-Microstructure, properties and applications, ISBN 1 85573 318 8, Abington Publishing, Cambridge, UK.

Keichel J et al, 2003, Deformation and Annealing Behavior of Nitrogen Alloyed Duplex Stainless Steels. Part I: Rolling, ISIJ Int, vol. 43, pp. 1781-1787.

Dehghan M.A. et al, Microstructural evolution during hot deformation of duplex stainless steel, 2007, Mat. Sci. Tech., vol. 23, pp. 1478-1484.

Bhattacharjee P.P. et al, 2013, Evolution of microstructure and texture during warm-rolling of a duplex steel, Metall. Mater. Trans. A, (inpress).

Latanision R.M. et al, 1971, the temperature dependence of stacking fault energy in Fe-Cr-Ni alloys, Metall Trans., vol. 2, pp. 505-509.

Smallman R.E. et al, 1964, dependence of rolling texture on stacking fault energy, Acta Metall., vol. 12, pp. 145-154.